Supplementary materials for:

Volcanogenic CO_2 degassing in the Songliao continental rift system, NE China

Wenbin Zhao [1, 2, 3], Zhengfu Guo [1, 2, 3 *], Ming Lei [1, 2, 3], Maoliang Zhang [1, 2, 3], Lin Ma [1, 2, 3], Danielle Fortin [4], Guodong Zheng [5, 6]

1. Key Laboratory of Cenozoic Geology and Environment, Institute of Geology and Geophysics, Chinese Academy of Sciences, Beijing 100029, China;

2. CAS Center for Excellence in Life and Paleoenvironment, Beijing, 100044, China;

3. College of Earth and Planetary Sciences, University of Chinese Academy of Sciences, Beijing 100049, China;

4. Department of Earth and Environmental Sciences, University of Ottawa, Ottawa, Ontario, K1N 6N5, Canada;

5. Northwest Institute of Eco-Environment and Resources, Chinese Academy of Sciences, Lanzhou 730000, China;

6. Key Laboratory of Petroleum Resources, Gansu Province, Lanzhou 730000, China

---

Contents

Supplementary Table S1 Measured soil CO_2 fluxes (g m^{-2} d^{-1}) of whole Wudalianchi monogenetic volcanic field, NE China.

Points	Latitude (N)	Longitude (E)	Slope	φ (g m^{-2} d^{-1})	Soil Temperature (°C)
1	48.6366	126.1071	0.154	1.81	22.8
2	48.6531	126.0634	4.078	47.83	21.2
3	48.6559	126.0556	0.837	9.82	21.7
4	48.7228	126.0296	0.501	5.88	23.3
5	48.7375	126.0467	0.654	7.67	23.0
6	48.7881	126.2606	0.799	9.37	27.3
7	48.7090	126.1256	0.351	4.12	22.5
8	48.7100	126.1233	0.253	2.97	27.0
9	48.7160	126.1273	0.800	9.38	22.3
10	48.7175	126.1270	0.580	6.80	20.1
11	48.7187	126.1246	1.445	16.94	18.1
12	48.7206	126.1237	1.375	16.13	18.2
13	48.7219	126.1203	0.953	11.18	22.8
14	48.6523	126.1339	1.420	16.66	25.0
15	48.6527	126.1342	5.611	65.82	24.3
16	48.6532	126.1358	1.137	13.34	23.3
17	48.6528	126.1347	10.859	127.38	23.0
18	48.6526	126.1341	5.498	64.49	28.7
19	48.6517	126.1329	1.975	23.16	23.3
20	48.6513	126.1323	1.879	22.05	28.5
21	48.6510	126.1313	0.299	3.51	27.0
22	48.6593	126.1293	2.770	32.49	29.8
23	48.6575	126.1268	0.268	3.15	27.9
24	48.6732	126.1225	0.305	3.58	27.9
25	48.6668	126.1250	4.346	50.98	28.7
26	48.6670	126.1262	7.203	84.50	32.3
27	48.6674	126.1275	6.471	75.91	33.0
28	48.6682	126.1300	2.842	33.34	33.3
29	48.6781	126.1161	0.291	3.42	29.6
30	48.6784	126.1251	2.494	29.26	30.5
31	48.6770	126.1258	1.733	20.33	31.7
32	48.6831	126.1128	2.597	30.47	27.7
33	48.6862	126.1032	2.824	33.12	30.3
34	48.6837	126.0986	6.518	76.45	22.5
35	48.6814	126.0910	0.852	10.00	29.4
36	48.6809	126.0888	6.835	80.18	23.3
37	48.6906	126.0911	2.282	26.77	26.8
38	48.6930	126.0828	0.367	4.31	29.7
39	48.7010	126.0605	2.032	23.84	29.8
40	48.7002	126.0607	7.926	92.97	30.1

41	48.6995	126.0606	0.485	5.69	29.9
42	48.6705	126.1131	1.483	17.39	31.1
43	48.6534	126.1364	13.769	161.50	23.5
44	48.6382	126.1039	0.626	7.34	26.4
45	48.6410	126.0964	4.887	57.33	25.7
46	48.6449	126.0878	0.448	5.25	28.5
47	48.6478	126.0797	0.202	2.37	28.5
48	48.6572	126.1349	1.177	13.81	22.8
49	48.6575	126.1194	0.410	4.80	21.5
50	48.6595	126.1322	1.032	12.11	18.8
51	48.6567	126.1151	0.242	2.83	20.7
52	48.6624	126.1100	0.187	2.20	20.4
53	48.6321	126.1719	0.342	4.01	19.5
54	48.6403	126.1670	0.232	2.73	18.7
55	48.6362	126.1484	0.417	4.89	18.4
56	48.6301	126.1448	0.476	5.59	19.2
57	48.6309	126.1530	0.202	2.37	20.5
58	48.6386	126.1330	0.349	4.09	20.8
59	48.6373	126.1342	0.681	7.99	18.8
60	48.6514	126.0751	0.220	2.58	20.8
61	48.6617	126.0312	0.176	2.06	21.5
62	48.6777	126.0158	0.534	6.26	22.5
63	48.6810	126.0327	0.413	4.85	22.8
64	48.7009	126.0087	0.231	2.71	21.8
65	48.7443	125.9928	0.214	2.51	19.6
66	48.7229	126.0188	0.959	11.25	23.2
67	48.7584	126.0647	0.242	2.83	22.8
68	48.7063	126.0403	0.262	3.07	23.6
69	48.6601	126.1700	0.162	1.90	25.6
70	48.6703	126.1947	0.220	2.58	19.8
71	48.6933	126.2130	0.412	4.83	21.2
72	48.6964	126.2271	0.268	3.14	22.5
73	48.7025	126.2263	0.417	4.89	25.3
74	48.7156	126.2345	3.672	43.07	23.6
75	48.7363	126.2371	0.500	5.87	23.4
76	48.7878	126.2482	0.382	4.48	21.6
77	48.6999	126.2564	0.419	4.91	23.2
78	48.6879	126.2856	0.995	11.67	24.1
79	48.6817	126.3084	0.284	3.33	23.5
80	48.6487	126.1388	0.315	3.69	24.5
81	48.6502	126.1374	0.341	4.00	22.1
82	48.6498	126.1362	0.451	5.29	23.2
83	48.6497	126.1344	0.310	3.64	22.8
84	48.6641	126.3222	0.325	3.81	23.8

85	48.6587	126.3297	0.297	3.49	25.5
86	48.7366	126.1589	1.734	20.37	20.2
87	48.7125	126.1295	0.280	7.96	25.6
88	48.7129	126.1289	0.175	4.88	17.5
89	48.7127	126.1287	0.096	2.69	22.8
90	48.7124	126.1287	0.166	4.62	18.6
91	48.7174	126.1398	0.385	10.85	26.6
92	48.7163	126.1409	0.304	8.36	25.0

Supplementary Table S2 Measured soil CO_2 fluxes (g m^{-2} d^{-1}) of SE slope of the Laoheishan volcanic cone.

Points	Latitude (N)	Longitude (E)	φ (g m^{-2} d^{-1})
W1	48.7101	126.1185	3.82
W2	48.7099	126.1186	2.50
W3	48.7096	126.1187	29.96
W4	48.7094	126.1188	4.37
W5	48.7103	126.1209	11.68
W6	48.7090	126.1199	12.18
W7	48.7096	126.1231	6.34
W8	48.7095	126.1237	17.90
W9	48.7099	126.1233	1.49
W10	48.7100	126.1231	4.66
W11	48.7100	126.1226	3.14
W12	48.7108	126.1226	54.06
W13	48.7107	126.1225	92.24
W14	48.7101	126.1221	11.77
W15	48.7092	126.1202	11.79
W16	48.7096	126.1201	4.17
W17	48.7099	126.1200	3.72
W18	48.7100	126.1211	3.11
W19	48.7104	126.1210	24.30
W20	48.7106	126.1209	6.46
W21	48.7107	126.1206	13.19
W22	48.7108	126.1208	7.56
W23	48.7109	126.1209	42.93
W24	48.7110	126.1210	7.18
W25	48.7109	126.1212	12.64
W26	48.7111	126.1212	5.69
W27	48.7112	126.1210	10.18
W28	48.7113	126.1208	11.92
W29	48.7111	126.1204	9.28
W30	48.7109	126.1202	11.67

W31	48.7107	126.1203	5.83
W32	48.7107	126.1233	31.62
W33	48.7097	126.1218	3.01
W34	48.7108	126.1186	7.96
W35	48.7105	126.1188	4.88
W36	48.7091	126.1226	2.69
W37	48.7093	126.1211	4.62
W38	48.7105	126.1196	6.31

Supplementary Table S3 Chemical and C-He isotope compositions of spring gases in WMVF

Sample No.	T (°C)	N_2 (%)	O_2 (%)	Ar (%)	CO_2 (%)	CH_4 (%)	He (ppm)	$^4He/^{20}Ne$	R_M/R_A	R_C/R_A	$\delta^{13}C$ (‰)	$CO_2/^3He$ ($\times10^9$)	Reference
Bubble gas samples from South spring													
NY17	9.2	7.96	0.35	0.16	91.1	0.07	129	182	2.64	2.64	-7.2	1.9	This study
NY18	7.7	8.73	0.55	0.18	90.5	0.14	278	153	3.10	3.10	-5.6	0.8	This study
NY1	5.1	/	/	/	/	/	/	10	3.87	3.95	-6.4	0.7	Mao et al., 2009
NY2	5.1	/	/	/	/	/	/	1	2.79	3.24	-7.0	10.8	Mao et al., 2009
SS	/	/	/	/	/	/	/	42	3.54	3.56	/	/	Shangguan, 2006
NYQ	/	2.13	0.00	0.07	97.8	0.00	8	55	3.25	3.26	-5.1	27.0	Du et al., 1999
NYQ−S	3.6	38.32	3.07	0.71	54.6	0.33	1540	42	3.51	3.53	/	0.1	Sun, 2008
Bubble gas samples from North spring													
BY17	7.8	3.42	0.32	0.06	95.8	0.10	379	685	2.26	2.26	-7.3	0.8	This study
BY18	6.5	3.22	0.25	0.07	96.5	0.38	18	40	3.16	3.17	-6.0	12.1	This study
BY1	8.2	4.60	1.13	0.10	94.0	0.11	9	4	2.64	2.74	-6.5	28.5	Mao et al., 2009
NS	4.7	/	/	/	/	/	/	47	3.11	3.13	-5.0	/	Shangguan, 2006
BYQ−S	4.7	8.63	1.43	0.26	86.5	1.05	60	67	3.09	3.10	-5.0	3.3	Sun, 2008
Bubble gas samples from Hualin spring													
HL17	19.8	4.61	0.88	0.08	94.1	0.02	10	38	2.34	2.35	-5.0	29.5	This study
HL18	24.0	4.90	1.29	0.09	93.7	0.04	433	72	2.97	2.98	-2.6	0.5	This study
HS	17.0	/	/	/	99.4	0.01	170	1860	3.03	3.03	-4.8	1.4	Xu et al., 2013
HL2	17.7	2.96	0.62	0.11	81.5	14.82	12	3	2.60	2.76	-5.3	18.8	Mao et al., 2009
HL1	17.7	2.28	1.04	0.06	96.4	0.04	230	232	3.06	3.06	-4.5	1.0	Mao et al., 2009
Hualin	17.6	/	/	/	/	/	/	46	3.20	3.22	-4.2	/	Shangguan, 2006
HLQ	/	11.98	2.84	0.16	85.0	0.00	150	103	3.27	3.28	-4.6	1.2	Du et al., 1999
HLFQ−S	17.6	2.82	0.80	0.07	96.5	/	340	5	3.18	3.31	-4.2	0.6	Sun, 2008
Bubble gas samples from Fanhua spring													
FH17	12.7	15.79	3.66	0.25	80.2	0.08	718	145	2.81	2.81	-4.3	0.3	This study
FH18	16.0	22.63	0.21	0.43	76.7	0.89	1845	359	3.18	3.18	-2.5	0.1	This study
FH2	5.3	16.76	0.70	0.40	82.0	0.14	35	157	3.30	3.30	-8.2	5.1	Mao et al., 2009
FH1	5.3	/	/	/	/	/	/	3	3.04	3.22	-8.8	1.5	Mao et al., 2009
FHQ	/	10.65	4.55	0.24	84.5	0.02	380	207	3.26	3.26	/	0.5	Du et al., 1999
Gas samples from other spring clusters in WMVF													

SG1	/	4.90	1.47	0.08	93.4	0.02	248	135	3.05	3.06	-4.5	0.9	Shangguan, 2008
SG2	/	7.64	1.08	0.17	90.2	0.38	126	37	3.03	3.05	-6.6	1.7	Shangguan, 2008
YQ	3.1	/	/	/	95.0	0.01	540	49	3.05	3.06	-3.1	0.4	Xu et al., 2013
WBQ	15.1	/	/	/	99.5	0.04	4	6	1.88	1.92	-5.8	97.6	Xu et al., 2013
DZT	/	2.76	0.53	0.05	96.6	0.01	110	1011	2.78	2.78	-7.4	2.3	Du et al., 1999

Supplementary Table S4 Reference values for associated parameters of DMM, CAR, ORS and COS end–members used in C–He isotope systematics.

End-member	$\delta^{13}C_{CO2}$ (‰)	C contents (ppm)	$^3He/^4He$ (R_A)	He contents (ppm)	$CO_2/^3He$ (*10^9)
DMM	–6.5[a]	1920[b]	8[a]	0.0288[b]	1.5[a]
CAR	0[c]	11400[d]	0.05[e]	0.00023[d]	1000~100000[f]
ORS	–18.5[g]	12618[j]	0.05[e]	0.0667[j]	1000~100000[f]
COS	–11[h]	Unknown	0.02[i]	Unknown	0.1~100000[f]

a. Sano and Marty (1995); b. Zhang et al. (2017); c. Hoefs (2009); d. Van Soest et al. (1998); e. Andrews (1985); f. O'Nions and Oxburgh (1988); g. Cook-Kollars et al. (2014); h. Hoefs and Frey (1976); i. Lupton (1983); j. Calculated based on U-Th decay.

*Helium content of the ORS end–member was calculated by on the U–Th decay of the Global subducting sediments (GLOSS) with accumulated age of 2.2 Ga (Wang et al., 2017). The contents of U and Th for the ORS end–member of GLOSS are from Plank and Langmuir (1998), Which are 2.62 ppm and 0.58 ppm, respectively (Mariana drill sites as a representative). The half–life and relatively contents of U and Th were also shown: $T_{1/2}(^{238}U)$ = 4.468 Ga, 99.2739%; $T_{1/2}(^{235}U)$ = 0.70381 Ga, 0.7024%; $T_{1/2}(^{232}Th)$ = 14.01 Ga, 100%, respectively (Steiger and Jager, 1977). We assume [He] equal to [^{4}He], the calculation formulas for Helium contents of the ORS end–member are presented as follows,

$$^{238}U \xrightarrow{8\alpha+6\beta} {}^{206}_{82}Pb + 8{}^4_2He + 6\beta^- + \mathrm{E}$$

$$^{235}U \xrightarrow{7\alpha+4\beta} {}^{207}_{82}Pb + 7{}^4_2He + 4\beta^- + \mathrm{E}$$

$$^{232}Th \xrightarrow{6\alpha+4\beta} {}^{208}_{82}Pb + 6{}^4_2He + 4\beta^- + \mathrm{E}$$

Helium concentrations:

$$[\mathrm{He}] = [\frac{^{238}U}{238} \times (e^{\frac{t*Ln2}{T_{\frac{1}{2}}}} - 1) \times 8 + \frac{^{235}U}{235} \times (e^{\frac{t*Ln2}{T_{\frac{1}{2}}}} - 1) \times 7 + \frac{^{232}U}{232} \times (e^{\frac{t*Ln2}{T_{\frac{1}{2}}}} - 1) \times 6] \times 4$$

Carbon concentration of ORS end–member was calculated by optimal K coefficient (K = 1.711) of CP (Carbonated Peridotite) and ORS, where K represents the ratio of He/C values between CP and ORS end–members.

Supplementary Table S5 Result of the C–He isotope systematics of the slab-mantle interactions of WMVF volatiles in the upper mantle beneath WMVF (stage 1, Figure 10).

DMM–CAR	8%	10%	13%	20%	40%	60%	80%
$^{3}He/^{4}He$ (R_A)	7.99	7.99	7.99	7.98	7.96	7.91	7.75
$\delta^{13}C$ (‰)	–4.29	–3.92	–3.44	–2.62	–1.31	–0.66	–0.27
He content (ppm)	0.027	0.026	0.025	0.023	0.017	0.012	0.006
C contents (ppm)	2868	2868	3152	3816	5712	7608	9504
CP–ORS	5%	10%	11%	13%	15%	20%	30%
$^{3}He/^{4}He$ (R_A)	7.05	6.23	6.08	5.79	5.51	4.88	3.83
$\delta^{13}C$ (‰)	–6.66	–8.70	–9.05	–9.70	–10.29	–11.56	–13.45
He content (ppm)	0.028	0.030	0.030	0.031	0.032	0.034	0.038
C contents (ppm)	3356	3843	3941	4136	4331	4818	5793

Supplementary Table S6 Result of the C–He isotope mixing between EM source and different proportions of continental crustal components (COS and CAR) of the WMVF volatiles during their ascending process (stage 2, Figure 10).

(COS: CAR)	(1:0)	(0.55:0.45)	(0.55:0.45)	(0.55:0.45)	(0.55:0.45)	(0.18:0.82)
EM: CRUST	0.7:0.3	0.7:0.3	0.6:0.4	0.5:0.5	0.4:0.6	0.7:0.3
$^{3}He/^{4}He$ (R_A)	2.43	3.29	2.65	2.10	1.60	4.62
$\delta^{13}C$ (‰)	–10.55	–8.21	–7.96	–7.78	–7.62	–5.81
He content (ppm)	0.053	0.039	0.041	0.044	0.046	0.027
C contents (ppm)	8300	7406	8497	9587	10677	6672
(COS: CAR)	(0.18:0.82)	(0.18:0.82)	(0.18:0.82)	(0:1)	(0:1)	(0:1)
EM: CRUST	0.6:0.4	0.5:0.5	0.4:0.6	0.4:0.6	0.2:0.8	0.1:0.9
$^{3}He/^{4}He$ (R_A)	4.16	3.65	3.08	5.73	5.62	5.43
$\delta^{13}C$ (‰)	–5.10	–4.53	–4.07	–1.89	–0.81	–0.38
He content (ppm)	0.026	0.025	0.024	0.013	0.006	0.003
C contents (ppm)	7518	8279	9209	8494	9947	10674

Supplementary Table S7 Reference values for associated parameters of DMM, CAR and ORS end–members used in Nd–Mg isotope mixing calculation.

End–member	$\delta^{26}Mg$ (‰)	MgO (%)	ε Nd (t)	Nd contents (ppm)
DMM	–0.25[a]	11.2[b]	+8[c]	7.3[d]
CAR	–2.51[e]	12.6[f]	+4[g]	500[g]
ORS*	–0.25[h]	3.59[i]	–18.1[j]	46[j]

a. Teng et al. (2010); b. Langmuir et al. (1977); c. Zindler and Hart (1986); d. Sun and McDonough (1989); e. Wang

et al. (2014); f. Hoernle et al. (2002); g. Bizimis et al. (2003); h. Wang et al. (2017); i. Plank and Langmuir (1998); j. Kuritani et al. (2011).

* Proterozoic sediments are assumed to represent the ORS (SIL) end–member, see details in Kuritani et al. (2011).

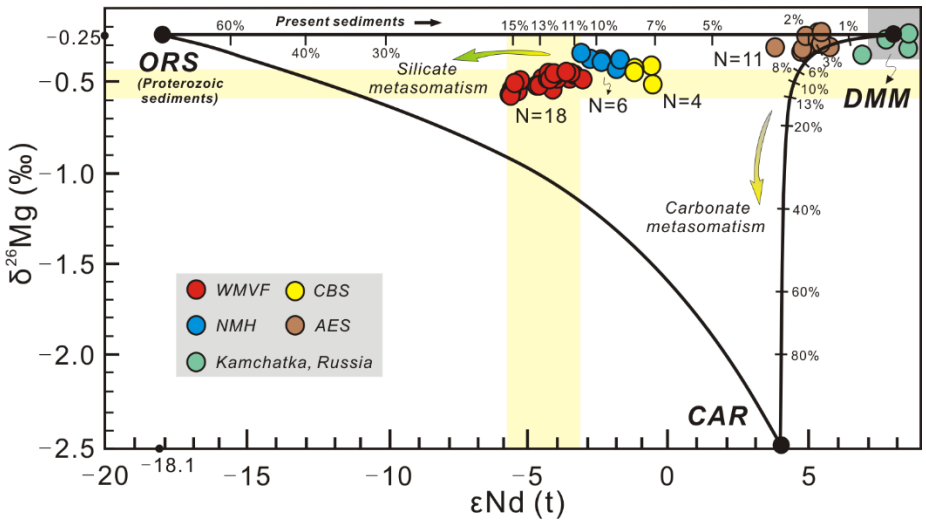

Supplementary Figure S1 Nd–Mg isotope mixing calculation for the typical Cenozoic basalts in NE China (Figure 1(a)). Abbreviations and references are as follows: WMVF, Wudalianchi monogenetic volcanic field; CBS, Changbaishan volcanic field; NMH, Nuominhe volcanic field; AES, Aershan volcanic field. Nd–Mg isotope data of these Cenozoic volcanic fields are from Li et al. (2016), Tian et al. (2016) and Wang et al. (2017).

Supplementary Table S8 Result of the Nd–Mg isotope calculation of silicate (ORS) and carbonate (CAR) metasomatism in the upper mantle beneath WMVF (Figure S1).

Degree of silicate metasomatism (%)	2	5	7	10	11	13	15	30	40	60
δ^{26}Mg (‰)	–0.25	–0.25	–0.25	–0.25	–0.25	–0.25	–0.25	–0.25	–0.25	–0.25
ε Nd (t)	5.03	1.50	–0.40	–2.75	–3.43	–4.66	–5.74	–11.05	–13.08	–15.61
MgO (%)	11.05	10.82	10.67	10.44	10.36	10.21	10.06	8.92	8.16	6.63
Nd contents (ppm)	8.07	9.24	10.01	11.17	11.56	12.33	13.11	18.91	22.78	30.52
Degree of carbonate metasomatism (%)	1	3	6	8	10	13	20	40	60	80
δ^{26}Mg (‰)	–0.28	–0.33	–0.40	–0.45	–0.50	–0.58	–0.75	–1.21	–1.67	–2.09
ε Nd (t)	6.36	5.28	4.74	4.58	4.46	4.36	4.22	4.09	4.04	4.01
MgO (%)	11.21	11.24	11.28	11.31	11.34	11.38	11.48	11.76	12.04	12.32
Nd contents (ppm)	12.23	22.08	36.86	46.72	56.57	71.35	105.84	204.38	302.92	401.46

Reference:

Andrews JN (1985) The isotopic composition of radiogenic helium and its use to study groundwater movement in confined aquifers. *Chemical Geology*, 49, 339–351.

Bizimis M, Salters VJM, Dawson JB (2003) The brevity of carbonatite sources in the mantle: evidence from Hf isotopes. *Contributions to Mineralogy and Petrology*, 145, 281–300.

Carapezza ML, Federico C (2000) The contribution of fluid geochemistry to the volcano monitoring of Stromboli. *Journal of Volcanology and Geothermal Research*, 95, 227–245.

Cook–Kollars J, Bebout GE, Collins NC, Angiboust S, Agard P (2014) Subduction zone metamorphic pathway for deep carbon cycling: Evidence from HP/UHP metasedimentary rocks, Italian Alps. *Chemical Geology*, 386, 31–48.

Di Martino RMR, Capasso G, Camarda M (2016) Spatial domain analysis of carbon dioxide from soils on Vulcano Island: Implications for CO_2 output evaluation. *Chemical Geology*, 444, 59–70.

Plank T, Langmuir CH (1998) The chemical composition of subducting sediment and its consequences for the crust and mantle. *Chemical Geology*, 145(3), 325–394.

Hernández PA, Pérez NM, Fridriksson T, Egbert J, Ilyinskaya E, Thárhallsson A, Ívarsson G, Gíslason G, Gunnarsson I, Jónsson B, Padrón E, Melián G, Mori T, Notsu K (2012) Diffuse volcanic degassing and thermal energy release from Hengill volcanic system, Iceland. *Bulletin of Volcanology*, 74, 2435–2448.

Hernández PA, Notsu K, Tsurumi M, Mori T, Ohno M, Shimoike Y, Salazar J, Pérez NM (2003) Carbon dioxide emissions from soils at Hakkoda, north Japan. *Journal of Geophysical Research*, 108, 2210.

Hoefs J (2009) Stable Isotope Geochemistry. Springer–Verlag, Berlin, Heidelberg.

Hoernle K, Tilton G, Le Bas M, Duggen S GarbeSchonberg D (2002) Geochemistry of oceanic carbonatites compared with continental carbonatites: mantle recycling of oceanic crustal carbonate. *Contributions to Mineralogy and Petrology*, 142, 520–542.

Kuritani T, Ohtani E, Kimura JI (2011) Intensive hydration of the mantle transition zone beneath China caused by ancient slab stagnation. *Nature Geoscience*, 4(10), 713–716.

O'Nions RK, Oxburgh ER (1988) Helium, volatile fluxes and the development of continental crust. *Earth and Planetary Science Letters*, 90, 331–347.

Sano Y, Marty B (1995) Origin of carbon in fumarolic gas from island arcs. *Chemical Geology*, 119, 265–274.

Steiger RH, Jager E (1977) Subcommission on geochronology: convention on the use of decay constants in geo– and cosmochronology. *Earth and Planetary Science Letters*, 36(3), 359–362.

Teng FZ, Li WY, Ke S, Marty B, Dauphas N, Huang S, Wu FY, Pourmand A (2010) Magnesium isotopic composition of the Earth and chondrites. *Geochimica et Cosmochimica Acta*, 74, 4150–4166.

Tian HC, Yang W, Li SG, Ke S, Chu ZY (2016) Origin of low δ^{26}Mg basalts with EM–I component: Evidence for interaction between enriched lithosphere and carbonated asthenosphere. *Geochimica et Cosmochimica Acta*, 188, 93–105.

Langmuir CH, Bender JF, Bence AE, Hanson GN, Taylor SR (1977) Petrogenesis of basalts from the FAMOUS area: Mid–Atlantic Ridge. *Earth and Planetary Science Letters*, 36(1), 133–156.

Li SG, Yang W, Ke S, Meng XN, Tian HC, Xu LJ, He YS, Huang J, Wang XC, Xia QC, Sun WD, Yang XY, Ren ZY, Wei HQ, Liu YS, Meng FC, Yan J (2016) Deep carbon cycles constrained by a large–scale mantle Mg isotope anomaly in eastern China. *National Science Review*, 4(1), 111–120.

Notsu K, Sugiyama K, Hosoe M, Uemura A, Shimoike Y, Tsunomori F, Sumino H, Yamamoto J, Mori T, Hernández PA (2005) Diffuse CO_2 efflux from Iwojima volcano, Izu–Ogasawara arc, Japan. *Journal of Volcanology and Geothermal Research*, 139, 147–161.

Sun SS, McDonough WF (1989) Chemical and isotopic systematics of oceanic basalts: implications for mantle composition and processes. In: Saunders AD, Norry MJ (ed.), *Magmatism in the Ocean Basins*, Geological Society, Special Publications, London, 42, 313–345.

Van Soest MC, Hilton DR, Kreulen R (1998) Tracing crustal and slab contributions to arc magmatism in the Lesser Antilles island arc

using helium and carbon relationships in geothermal fluids. *Geochimica et Cosmochimica Acta*, 62, 3323–3335.

Wang XJ, Chen LH, Hofmann AW, Mao FG, Liu JQ, Zhong Y, Xie LW, Yang YH (2017) Mantle transition zone–derived EM1 component beneath NE China: Geochemical evidence from Cenozoic potassic basalts. *Earth and Planetary Science Letters*, 465, 16–28.

Wang SJ, Teng FZ, Li SG (2014) Tracing carbonate–silicate interaction during subduction using magnesium and oxygen isotopes. *Nature Communications*, 5(1), 5328.

Wang XJ, Chen LH, Hofmann AW, Mao FG, Liu JQ, Zhong Y, Xie LW, Yang YH (2017) Mantle transition zone–derived EM1 component beneath NE China: Geochemical evidence from Cenozoic potassic basalts. *Earth and Planetary Science Letters*, 465, 16–28.

Werner C, Hurwitz S, Evans W C, Lowenstern J B, Bergfeld D, Heasler H, Jaworowski C, Hunt A (2008) Volatile emissions and gas geochemistry of Hot Spring Basin, Yellowstone National Park, USA. *Journal of Volcanology and Geothermal Research*, 178(4), 751–762.

Zhang LH, Guo ZF, Sano Y, Zhang ML, Sun YT, Cheng ZH, Yang TF (2017) Flux and genesis of CO_2 degassing from volcanic–geothermal fields of Gulu–Yadong rift in the Lhasa terrane, South Tibet: Constraints on characteristics of deep carbon cycle in the India–Asia continent subduction zone. *Journal of Asian Earth Sciences*, 149, 110–123.

Zhang ML, Guo ZF, Sano Y, Cheng ZH, Zhang LH (2015) Stagnant subducted Pacific slab–derived CO_2 emissions: Insights into magma degassing at Changbaishan volcano, NE China. *Journal of Asian Earth Sciences*, 106, 49–63.

Zhang ML, Guo ZF, Sano Y, Zhang LH, Sun YT, Cheng ZH, Yang TF (2016) Magma–derived CO_2 emissions in the Tengchong volcanic field, SE Tibet: Implications for deep carbon cycle at intra–continent subduction zone. *Journal of Asian Earth Sciences*, 127, 76–90.

Zindler A, Hart S (1986) Chemical geodynamics. *Annual Review of Earth and Planetary Science*, 14, 493–571.